PHYSICAL REVIEW B **73**, 241311(R) (2006)

Weak antilocalization in gate-controlled $Al_xGa_{1-x}N/GaN$ two-dimensional electron gases

N. Thillosen, S. Cabañas, N. Kaluza, V. A. Guzenko, H. Hardtdegen, and Th. Schäpers*
Institute of Thin Films and Interfaces (ISG 1) and Virtual Institute of Spin Electronics (VISel), Research Centre Jülich GmbH, 52425 Jülich, Germany

(Received 2 March 2006; revised manuscript received 11 April 2006; published 20 June 2006)

Weak antilocalization and the Shubnikov–de Haas effect were investigated in $Al_xGa_{1-x}N/GaN$ two-dimensional electron gases. The weak antilocalization measurements on a gated sample revealed a constant spin-orbit scattering length, which does not change if the Al content or the thickness of the $Al_xGa_{1-x}N$ barrier layer is varied. The occurrence of spin-orbit coupling is assigned to the lack of crystal inversion symmetry. Although for some of the samples a beating pattern was observed in the Shubnikov–de Haas oscillations, its presence was not attributed to spin-orbit coupling but rather to inhomogeneities in the $Al_xGa_{1-x}N$ barrier.

DOI: 10.1103/PhysRevB.73.241311 PACS number(s): 73.43.Qt, 72.25.Rb, 73.20.Fz, 73.61.Ey

The interest in GaN-based semiconductors for future spintronic applications is motivated by two aspects: First, nitride-based diluted magnetic semiconductors are promising candidates for spin injector or spin analyzer electrodes, since for this material system Curie temperatures above room temperature are theoretically expected and experimentally reported (see, e.g., Ref. 1, and references therein). Second, two-dimensional electron gases (2DEGs) in $Al_xGa_{1-x}N/GaN$ layer systems are potential candidates for gate-controlled spin precession utilizing the Rashba effect.[2–5]

Spin-orbit coupling in a 2DEG can be studied by analyzing the characteristic beating pattern in the Shubnikov–de Haas oscillations. Information on the magnitude of the spin splitting due to spin-orbit coupling can be obtained from the node positions in the beating pattern.[6,7] Also the control of the spin-orbit coupling can be confirmed by changing the gate voltage, which changes the shape of the confining potential.[8,9] Alternatively, spin-orbit coupling in a 2DEG can be studied by analyzing quantum correction to the conductance; i.e., weak antilocalization (WAL) (Refs. 10–12). In contrast to the weak localization effect (WL), where the conductance is decreased owing to constructive interference between time reversed paths, random deviations of the spin orientations due to spin-orbit coupling result in an enhanced conductance.[13,14] The control of the spin-orbit coupling can also be studied by means of WAL experiments.[15–17]

In wurtzite-type $Al_xGa_{1-x}N/GaN$ 2DEGs zero-field spin splitting can originate from two mechanisms. First, it can be due to a macroscopic electric field in an asymmetric quantum well containing the 2DEG (*interface* Rashba effect).[2] If this is the case, the strength of the spin-orbit coupling can be controlled by a gate voltage.[8,9] Second, the lack of inversion symmetry of the wurtzite-type lattice can result in a zero-field spin splitting as well. In contrast to zinc-blende-type lattices,[18] here the effective electric field is oriented along the (0001) direction and thus parallel to the macroscopic electric field in the quantum well (*bulk* Rashba effect).[19] Although spin-orbit coupling in $Al_xGa_{1-x}N/GaN$ 2DEGs had been studied intensively by analyzing the beating pattern in the Shubnikov–de Haas oscillations[20–23] or by measuring WAL (Ref. 24), its underlying mechanism is not yet fully understood. In this Rapid Communication we report on antilocalization studies and Shubnikov–de Haas measurements extended to gate-controlled $Al_xGa_{1-x}N/GaN$ 2DEGs. We will have clear evidence on whether the spin-orbit coupling remains effectively constant or not. These studies are supplemented by measurements of two $Al_xGa_{1-x}N/GaN$ heterostructures with a different $Al_xGa_{1-x}N$ barrier layer. The experimental findings are interpreted by considering the different contributions to the spin-orbit coupling in $Al_xGa_{1-x}N/GaN$ 2DEGs.

The polarization-doped $Al_xGa_{1-x}N/GaN$ heterostructures were grown by metalorganic vapor phase epitaxy on a (0001) Al_2O_3 substrate. The layer sequences consisted of a 3-μm-thick GaN layer and an AlGaN top layer. Both layers were nominally undoped. Three different layer systems were investigated. Their Al contents, as well as their layer thicknesses, are given in Table I. By using dry mesa etching, 200 μm wide Hall bar structures with voltage probes separated by 180 μm were prepared. Ohmic contacts of Ti/Al/Ni/Au were annealed at 900 °C for 30 s. Sample 1 was covered by a Ni/Au gate electrode isolated from the semiconductor surface by a 30-nm-thick SiO_2 layer.

From Shubnikov–de Haas measurements at 1.0 K the electron concentrations n and mobilities μ were determined (Table I). An effective electron mass m^* of 0.22 m_e was extracted from temperature-dependent Shubnikov–de Haas measurements.

In Fig. 1(a) the magnetoresistance R_{xx} of sample 1 is shown for various gate voltages V_G. In the Shubnikov–de Haas oscillations a beating pattern is observed resulting in a double-peak structure in the $1/B$ fast Fourier transform (FFT) [Fig. 1(b)]. Only a single node is resolved in the beat-

TABLE I. Summary of parameters of the different samples: Al content x, thickness d of the AlGaN layer, electron concentration n, and mobility μ. The values of n and μ for sample 1 were taken at $V_G=0$.

Sample	x (Al)	d (AlGaN) (nm)	n@1.0 K (10^{12} cm^{-2})	μ@1.0 K (cm^2/V s)
1	0.15	35	4.21	7390
2	0.15	70	3.62	7580
3	0.30	30	8.00	6820

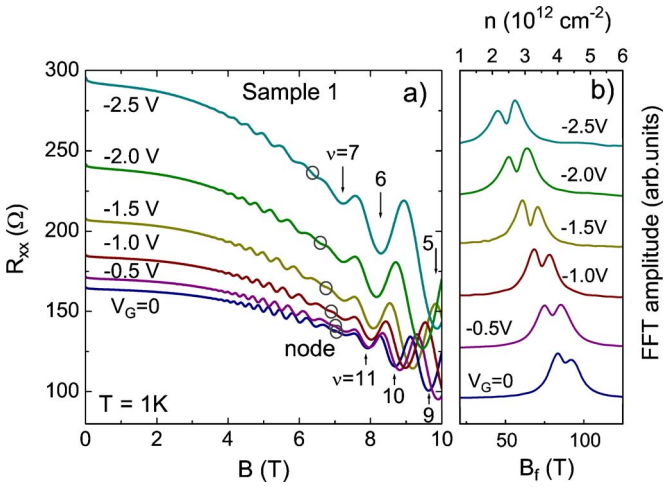

FIG. 1. (Color online) (a) Magnetoresistance R_{xx} of sample 1 for different gate voltages in the range from 0 to −2.5 V at 1.0 K. The node positions are indicated by circles. For $V_G=0$ and −2.5 V the filling factors ν are given. (b) Amplitude of the corresponding $1/B$ fast Fourier transform of the magnetoresistance in arbitrary units as a function of the oscillation frequency B_f in units of T. The corresponding electron concentration n is given by the upper scale.

ing pattern, which shifts from 7 T at $V_G=0$ to 6.3 T at −2.5 V. From the average position of the double-peak structure the electron concentration was extracted at each gate voltage. At zero gate voltage $n=4.2\times10^{12}$ cm^{-2} is found, which reduces to almost half its value of 2.4×10^{12} cm^{-2} at $V_G=-2.5$ V. The average electron concentration determined from the fast Fourier spectrum corresponds to n determined from the Hall measurements. Simultaneously, the mobility decreases from 7390 to 6990 cm^2/V s, respectively.

The presence of spin-orbit coupling can be deduced from the measurements of the magnetoconductivity $\sigma(B)-\sigma(0)$ shown in Fig. 2. Here, a peak is found at $B=0$ that can be attributed to WAL, whereas the increase for $|B|>2$ mT can

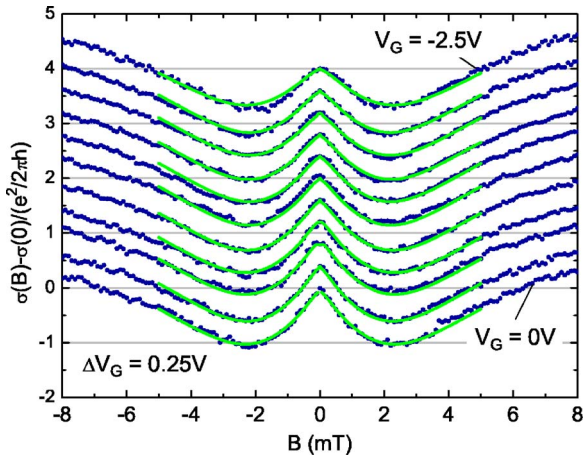

FIG. 2. (Color online) Experimental values (●) of the quantum correction to the conductivity $\sigma(B)-\sigma(0)$ in units of $e^2/2\pi h$ vs B of sample 1 at $T=1$ K. The gate voltage V_G was varied from 0 to −2.5 V in steps of 0.25 V. The curves are offset by 0.2 $e^2/2\pi h$ for clarity. Full lines show the fit to the experimental data using the ILP model (Ref. 25).

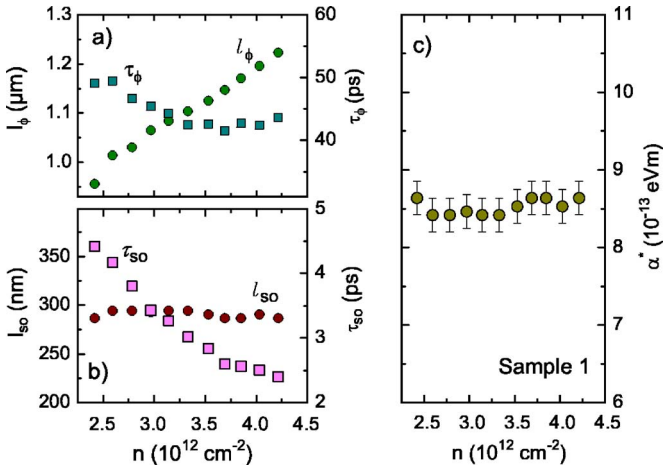

FIG. 3. (Color online) (a) Phase coherence length l_ϕ and phase coherence time τ_ϕ vs electron concentration n. (b) Spin-relaxation length l_{so} and spin-relaxation time τ_{so} vs n. The corresponding effective spin-orbit coupling parameter α^* is shown in (c).

be assigned to WL being the dominant contribution at larger magnetic fields. A WAL peak is found for all gate voltages. However, a slight peak height decrease is observed for increasing values of V_G.

In order to obtain information on the magnitude of the spin-orbit coupling at different gate voltages, the experimental curves were analyzed using the theory of Iordanskii, Lyanda-Geller, and Pikus (ILP) (Ref. 25). In this model the quantum conductance correction is quantified by three characteristic magnetic fields. The first one is $B_{tr}=\hbar/2el_{tr}^2$, with $l_{tr}=v_F\tau_{tr}$. Here, l_{tr} is the transport mean free path and v_F the Fermi velocity. The transport scattering times τ_{tr} at different gate voltages were determined from $\tau_{tr}=\mu m^*/e$. The second characteristic field, which is related to the phase coherence length l_ϕ, is defined as $B_\phi=\hbar/4el_\phi^2$. Here, l_ϕ is given by $\sqrt{D\tau_\phi}$, with $D=\frac{1}{2}v_F^2\tau_{tr}$ the diffusion constant and τ_ϕ the phase coherence time. The magnitude of the spin-orbit coupling is quantified by $B_{so}=\hbar/4el_{so}^2$, with $l_{so}=\sqrt{D\tau_{so}}$ the spin-relaxation length and τ_{so} the corresponding spin-relaxation time. Only the Rashba contribution was considered in the fit. The ILP model is valid in the diffusive regime where $B<B_{tr}$. For our set of measurements $B_{tr}\gtrsim5$ mT.

It can be seen in Fig. 2 that the experimental data of $\sigma(B)-\sigma(0)$ can be fitted very well by the ILP model. Since τ_{tr} and D are extracted directly from the Shubnikov–de Haas measurements, only B_ϕ and B_{so} had to be used as fit parameters. The height of the WAL peak at $B=0$ is closely related to B_ϕ and thus to the phase coherence length l_ϕ. The above mentioned larger peak heights for larger n can directly be related to an increased value of l_ϕ. As can be seen in Fig. 3(a), l_ϕ is increased from a value of 0.96 μm at $n=2.4\times10^{12}$ cm^{-2} ($V_G=-2.5$ V) to 1.22 μm at $n=4.2\times10^{12}$ cm^{-2} ($V_G=0$). In contrast, the corresponding phase coherence time τ_ϕ slightly decreases with n, as can be seen in Fig. 3(a). The fact that l_ϕ nevertheless increases with n can be explained by the increase of D with increasing n which overcompensates the effect of τ_ϕ. The experimental values of τ_ϕ are one order of magnitude larger than the values ex-

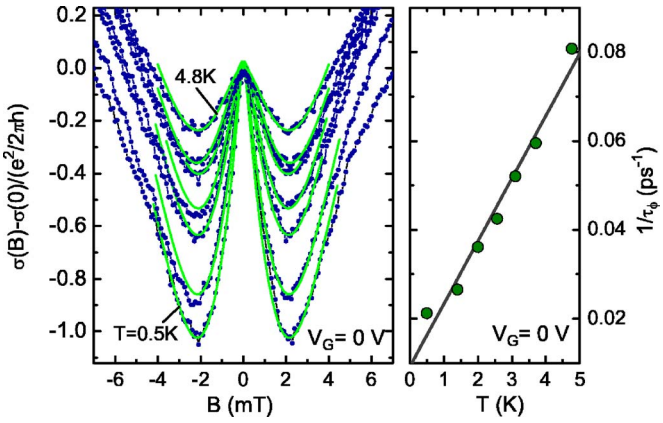

FIG. 4. (Color online) (a) Experimental values (●) of $\sigma(B)-\sigma(0)$ in units of $e^2/2\pi h$ vs B of sample 1 at $V_G=0$. From the top to the bottom, the curves correspond to $T=4.8, 3.7, 3.1, 2.6, 2.0, 1.4, 0.5$ K. Full lines (green) show the fit to the experimental data using the ILP model (Ref. 25). (b) Inverse phase coherence time $1/\tau_\phi$ as a function of temperature at $V_G=0$. The gray line shows the corresponding linear fit.

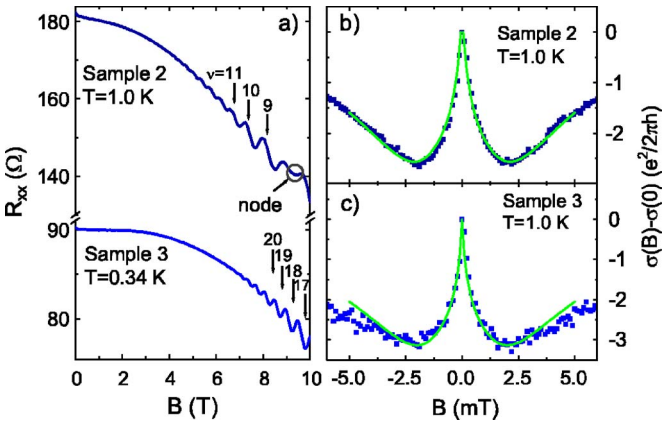

FIG. 5. (Color online) (a) Shubnikov–de Haas oscillations of samples 2 and 3. The filling factors ν are given for higher magnetic fields. Because of the beating pattern, ν has to be assigned to the maxima of the oscillations for sample 2. (b) Sample 2: Experimental values (●) of $\sigma(B)-\sigma(0)$ in units of $e^2/2\pi h$ vs B and fit to the ILP model (full line). (c) Corresponding data for sample 3.

pected from theory.[26] The large discrepancy might be due to the small Fermi energy of the 2DEG compared to metallic systems.[14,27]

Although in our set of measurements n is increased by almost a factor of 2, the spin-relaxation length l_{so} remains at about the same value of approximately 290 nm [Fig. 3(b)]. However, since D increases with n, τ_{so} does decrease with increasing electron concentration. Since we could not distinguish between the interface and bulk Rashba effect we calculated an effective spin-orbit coupling parameter comprising both contributions by:[16] $\alpha^*=\hbar^2/\sqrt{2}m^* l_{so}$. The value of α^* remains almost constant at 8.5×10^{-13} eV m for all gate voltages, since α^* depends only on l_{so} [see Fig. 3(c)].

The peak height in $\sigma(B)-\sigma(0)$ attributed to WAL is reduced if the temperature is increased, as can be seen in Fig. 4(a). By fitting the experimental data to the ILP model we found that this decrease can be explained solely by a reduction of l_ϕ with increasing temperature while l_{so} remains constant. As can be seen in Fig. 4(b), $1/\tau_\phi$ increases linearly with temperature in accordance with theoretical models.[26] Spin-orbit coupling mainly effects the position of the minima in $\sigma(B)-\sigma(0)$, which are found at approximately ±2 mT for all temperatures. Consequently, from the fit to the ILP model we found that B_{so} remains at the same value of 2 mT, corresponding to $l_{so}=290$ nm.

We have seen that for sample 1 the spin-relaxation length l_{so} is constant if the electron concentration or temperature is changed. An interesting question is whether a different value of l_{so} could be observed in $Al_xGa_{1-x}N/GaN$ 2DEGs with different layer sequences. For this reason, we investigated a layer system with a thicker barrier layer (sample 2) and a sample with a higher Al content of 30% in the barrier layer (sample 3). As can be seen in Figs. 5(b) and 5(c), for both samples the minima in $\sigma(B)-\sigma(0)$ are found at ±2 mT, resulting in the same spin-relaxation length as for sample 1. This result shows that l_{so} seems to be solely determined by the GaN channel layer and that it is not affected by the barrier.

Often information on the spin-orbit coupling parameter is extracted from the nodes in the beating pattern of the Shubnikov–de Haas oscillations. Assuming that the origin of the beating pattern can be attributed to Rashba spin splitting, the coupling parameter α^* was determined from a fit to calculated magnetoresistance oscillations. The latter is based on the energy spectrum including the Landau quantization, the Zeeman term, and the Rashba effect.[29] For the g factor a value of 1.95 was taken.[28] For sample 1 a value of $\alpha^*=4.7\times10^{-12}$ eV m was extracted at $V_G=0$, which monotonously increases to 5.7×10^{-12} eV m at $V_G=-2.5$ V. Interestingly, for sample 2 the node in the beating pattern is found at a higher magnetic field of 9 T compared to sample 1, resulting in $\alpha^*=6.5\times10^{-12}$ eV m [see Fig. 1(a)]. In contrast, for sample 3 no signature of a beating pattern is observed. Taking all three samples into consideration, it can be inferred that α^* extracted from the beating pattern is not consistent with α^* determined from the WAL analysis.

For a 2DEG with a single subband occupied, as in our case, the presence of WAL is an unambiguous sign of the presence of spin-orbit coupling. In contrast, a beating pattern in the Shubnikov–de Haas oscillations can have other origins, e.g., an inhomogeneous carrier distribution.[30] Cathodoluminescence spectroscopy of $Al_xGa_{1-x}N/GaN$ interface structures has shown that in the $Al_xGa_{1-x}N$ barrier layer domains with slightly different Al content can be formed.[31,32] This would result in a slightly different electron concentration in the 2DEG and under certain domain distributions to a beating pattern in the Shubnikov–de Haas oscillations. For our samples this interpretation might apply, since the signature of the beating pattern changes from sample to sample. For a definite answer concerning this issue further structural studies are required. In any case, the value of α^* extracted from the beating pattern is too large if compared to the values obtained from the WAL measurements. As shown above, α^* obtained from the WAL analysis is identical for all three samples under study, although the $Al_xGa_{1-x}N$ barrier layers as well as n are different. Furthermore, for sample 1 the

effective spin-orbit coupling parameter does not change with gate voltage. From this observation we can conclude that the contribution of the interface Rashba effect can be neglected. The spin-orbit scattering present in our sample thus seems to be completely determined by the bulk Rashba effect, which is a crystal effect and cannot be controlled by a gate.

In conclusion, spin-orbit coupling in $Al_xGa_{1-x}N/GaN$ 2DEGs was investigated. WAL measurements on a gated sample as well as on samples with different barrier layers revealed a constant effective spin-orbit coupling parameter. No evidence of the interface Rashba effect was found. The beating pattern observed in the Shubnikov–de Haas oscillations of some samples could not be attributed to the presence of spin-orbit coupling but rather to electron concentration variations due to inhomogeneities of the $Al_xGa_{1-x}N$ barrier layer.

The authors thank M. Marso (ISG-1) for performing the CV measurements and H. Kertz (ISG-1) for assistance during the low-temperature measurements. Fruitful discussions with R. Winkler (Northern Illinois University) and Yu. Lyanda-Geller (Purdue University) are gratefully acknowledged.

*Electronic address: th.schaepers@fz-juelich.de

[1] C. Liu, F. Yun, and H. Morkoç, J. Mater. Sci. **16**, 555 (2005).
[2] Y. Bychkov and E. I. Rashba, J. Phys. C **17**, 6039 (1984).
[3] R. Winkler, *Spin Orbit Coupling Effects in Two-dimensional Electron and Hole Systems* (Springer-Verlag, Berlin, 2003).
[4] V. I. Litvinov, Phys. Rev. B **68**, 155314 (2003).
[5] I. Lo, W. T. Wang, M. H. Gau, S. F. Tsay, and J. C. Chiang, Phys. Rev. B **72**, 245329 (2005).
[6] J. Luo, H. Munekata, F. F. Fang, and P. J. Stiles, Phys. Rev. B **38**, R10142 (1988).
[7] B. Das, D. C. Miller, S. Datta, R. Reifenberger, W. P. Hong, P. K. Bhattacharya, J. Singh, and M. Jaffe, Phys. Rev. B **39**, R1411 (1989).
[8] J. Nitta, T. Akazaki, H. Takayanagi, and T. Enoki, Phys. Rev. Lett. **78**, 1335 (1997).
[9] G. Engels, J. Lange, Th. Schäpers, and H. Lüth, Phys. Rev. B **55**, R1958 (1997).
[10] P. D. Dresselhaus, C. M. A. Papavassiliou, R. G. Wheeler, and R. N. Sacks, Phys. Rev. Lett. **68**, 106 (1992).
[11] W. Knap, C. Skierbiszewski, A. Zduniak, E. Litwin-Staszewska, D. Bertho, F. Kobbi, J. L. Robert, G. E. Pikus, F. G. Pikus, S. V. Iordanskii, V. Mosser, K. Zekentes, and Yu. B. Lyanda-Geller, Phys. Rev. B **53**, 3912 (1996).
[12] T. Hassenkam, S. Pedersen, K. Baklanov, A. Kristensen, C. B. Sorensen, P. E. Lindelof, F. G. Pikus, and G. E. Pikus, Phys. Rev. B **55**, 9298 (1997).
[13] S. Hikami, A. I. Larkin, and Y. Nagaoka, Prog. Theor. Phys. **63**, 707 (1980).
[14] G. Bergmann, Phys. Rep. **107**, 1 (1984).
[15] T. Koga, J. Nitta, T. Akazaki, and H. Takayanagi, Phys. Rev. Lett. **89**, 046801 (2002).
[16] C. Schierholz, R. Kürsten, G. Meier, T. Matsuyama, and U. Merkt, Phys. Status Solidi B **233**, 436444 (2002).
[17] J. B. Miller, D. M. Zumbühl, C. M. Marcus, Y. B. Lyanda-Geller, D. Goldhaber-Gordon, K. Campman, and A. C. Gossard, Phys. Rev. Lett. **90**, 076807 (2003).
[18] G. Dresselhaus, Phys. Rev. **100**, 580 (1955).
[19] E. I. Rashba, Fiz. Tverd. Tela (Leningrad) **2** 1224 (1960) [Sov. Phys. Solid State **2**, 1109 (1960)].
[20] I. Lo, J. K. Tsai, W. J. Yao, P. C. Ho, L. W. Tu, T. C. Chang, S. Elhamri, W. C. Mitchel, K. Y. Hsieh, J. H. Huang, H. L. Huang, and W. C. Tsai, Phys. Rev. B **65**, 161306(R) (2002).
[21] K. Tsubaki, N. Maeda, T. Saitoh, and N. Kobayashi, Appl. Phys. Lett. **80**, 3126 (2002).
[22] J. Lu, B. Shen, N. Tang, D. J. Chen, H. Zhao, D. W. Liu, R. Zhang, Y. Shi, Y. D. Zheng, Z. J. Qiu, Y. S. Gui, B. Zhu, W. Yao, J. H. Chu, K. Hoshino, and Y. Arakawa, Appl. Phys. Lett. **85**, 3125 (2004).
[23] K. Cho, T.-Y. Huang, H.-S. Wang, M.-G. Lin, T.-M. Chen, C.-T. Liang, and Y. F. Chen, Appl. Phys. Lett. **86**, 222102 (2005).
[24] N. Thillosen, Th. Schäpers, N. Kaluza, H. Hardtdegen, and V. A. Guzenko, Appl. Phys. Lett. **88**, 022111 (2006).
[25] S. V. Iordanskii, Y. B. Lyanda-Geller, and G. E. Pikus, JETP Lett. **60**, 206 (1994).
[26] B. L. Al'tshuler, A. G. Aronov, and D. E. Khmelnitsky, J. Phys. C **15**, 7367 (1982).
[27] S. A. Studenikin, P. T. Coleridge, P. Poole, and A. Sachrajda, JETP Lett. **77**, 311 (2003).
[28] M. W. Bayerl, M. S. Brandt, T. Graf, O. Ambacher, J. A. Majewski, M. Stutzmann, D. J. As, and K. Lischka, Phys. Rev. B **63**, 165204 (2001).
[29] M. Zarea and S. E. Ulloa, Phys. Rev. B **72**, 085342 (2005).
[30] S. Brosig, K. Ensslin, R. J. Warburton, C. Nguyen, B. Brar, M. Thomas, and H. Kroemer, Phys. Rev. B **60**, R13989 (1999).
[31] T. Riemann, J. Christen, A. Kaschner, A. Laades, A. Hoffmann, C. Thomsen, M. Iwaya, S. Kamiyama, H. Amano, and I. Akasaki, Appl. Phys. Lett. **80**, 3093 (2002).
[32] A. Bell, R. Liu, U. K. Parasuraman, F. A. Ponce, S. Kamiyama, H. Amano, and I. Akasaki, Appl. Phys. Lett. **85**, 3417 (2004).